Characteristics of seismic survey pulses and the ambient soundscape in Baffin Bay and Melville Bay, West Greenland

S. Bruce Martin,[a] Marie-Noël R. Matthews, and Jeff T. MacDonnell[b]
JASCO Applied Sciences (Canada) Ltd., 32 Troop Avenue, Suite 202, Dartmouth, Nova Scotia B3B 1Z1, Canada

Koen Bröker[c]
Shell Global Solutions International B.V., Lange Kleiweg 40, 2288GK Rijswijk, The Netherlands

(Received 28 August 2016; revised 3 October 2017; accepted 9 November 2017; published online 1 December 2017)

In 2012 a seismic survey campaign involving four vessels was conducted in Baffin Bay, West Greenland. Long-distance (150 km) pre-survey acoustic modeling was performed in accordance with regulatory requirements. Four acoustic recorders, three with hydrophones at 100, 200, and 400 m depths, measured ambient and anthropogenic sound during the survey. Additional recordings without the surveys were made from September 2013 to September 2014. The results show that (1) the soundscape of Baffin Bay is typical for open ocean environments and Melville Bay's soundscape is dominated by glacial ice noise; (2) there are distinct multipath arrivals of seismic pulses 40 km from the array; (3) seismic sound levels vary little as a function of depth; (4) high fidelity pre-survey acoustic propagation modeling produced reliable results; (5) the daily SEL did not exceed regulatory thresholds and were different using Southall, Bowles, Ellison, Finneran, Gentry, Greene, Kastak, Ketten, Miller, Nachtigall, Richardson, Thomas, and Tyack [(2007) Aquat. Mamm. **33**, 411–521] or NOAA weightings [National Marine Fisheries Service (2016). NOAA Technical Memorandum NMFS-OPR-55, p. 178]; (6) fluctuations of SPL with range were better described by additive models than linear regression; and (7) the survey increased the 1-min SPL by 28 dB, with most of the energy below 100 Hz; energy in the 16 000 Hz octave band was 20 dB above the ambient background 6 km from the source.
https://doi.org/10.1121/1.5014049

[JFL] Pages: 3331–3346

I. INTRODUCTION

In 2010, five petroleum exploration license blocks were awarded in Baffin Bay, West Greenland. Some of these blocks have considerable overlap with narwhal protection areas and are proximal to the Melville Bay Nature Reserve (Fig. 1). As part of the environmental permitting process for seismic surveys in Greenland, the Danish Centre for Environment and Energy (DCE) issued Environmental Impact Assessment requirements that include acoustic modeling and monitoring guidelines (Kyhn *et al.*, 2011). These guidelines define many of the responsible practices with respect to marine mammals and seismic surveys that were subsequently described by Nowacek *et al.* (2013). The main mitigation measures in these guidelines are (1) establishing the radius of exclusion zones with high-fidelity acoustic modeling; (2) visually and/or acoustically monitoring exclusion zones to minimize auditory injury to marine mammals; and (3) turning off active sources when mammals are detected in exclusion zones. The DCE guidelines (Kyhn *et al.*, 2011) apply the dual criteria recommended by Southall *et al.* (2007): a maximum peak sound pressure level (SPL) and a 24-h sound exposure level (SEL) limit. Seismic surveys are usually performed using arrays of airguns spread over an area on the order of 100 m^2 and are therefore not point sources. The range from an airgun array where the peak sound pressure level criterion of 230 dB re 1 μPa for cetaceans is exceeded (if at all) is at most on the order of tens of meters, indeed comparable to the size of the airgun array itself (Caldwell and Dragoset, 2000; Gisiner, 2016). Thus, the criterion of concern for defining exclusion zones is the 24-h SEL. The 24-h SEL thresholds recommended in Southall *et al.* (2007) are weighted for the hearing bands of mammal groups; the SEL criterion is typically exceeded at ranges from the airgun array on the order of hundreds of meters (e.g., Tashmukhambetov *et al.*, 2008; Breitzke and Bohlen, 2010; Matthews, 2012). It is widely accepted that applying mitigation zones based on these thresholds minimizes the risk of injuring marine mammals (Gordon *et al.*, 2003; Wartzok *et al.*, 2003; Southall *et al.*, 2007; Nowacek *et al.*, 2013).

Seismic airgun pulses can be perceptible above the background ocean sound at distances in the order of hundreds of kilometers (e.g., Bohnenstiehl *et al.*, 2012a; MacGillivray *et al.*, 2014; Blackwell *et al.*, 2015) and even farther if the energy propagates in a deep sound channel (Thode *et al.*, 2010; Nieukirk *et al.*, 2012; Blackwell *et al.*,

[a]Also at: Department of Oceanography, Dalhousie University, 1355 Oxford Street, P.O. Box 15000, Halifax, Nova Scotia B3H 4R2, Canada. Electronic mail: bruce.martin@jasco.com
[b]Current address: Acoustic Data Analysis Center, P.O. Box 99000, Stn Forces Halifax, Nova Scotia B3K 5X5, Canada.
[c]Also at: Groningen Institute for Evolutionary Life Sciences, University of Groningen, P.O. Box 11103, 9700 CC Groningen, The Netherlands.

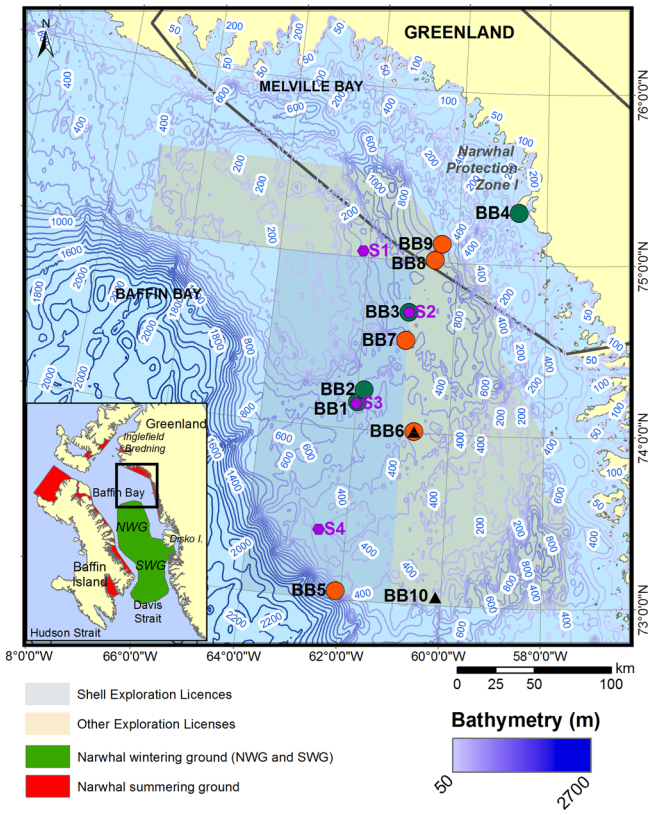

FIG. 1. (Color online) Recorder stations in summer 2012 (green circles/darker gray), summer 2013 (orange circles/lighter gray), and overwinter 2013–2014 (black triangles), as well as pre-survey modeling locations (purple hexagons). Narwhal protection area data from Kyhn *et al.* (2011).

2015). At ranges between the injury exclusion zones and the limits of perception for seismic sound, animals may experience temporary threshold shift (TTS), behavioral disturbance, and masking effects (Gordon *et al.*, 2003; Southall *et al.*, 2007; Nowacek *et al.*, 2013). The sound levels that induce behavioral responses from marine mammals cover a wide range of sound pressure and sound exposure levels and are dependent on factors such as the type of activity an animal was engaged in when exposed to the sound (e.g., Richardson *et al.*, 1986; Wartzok *et al.*, 2003; Ellison *et al.*, 2012; Robertson *et al.*, 2013). It is extremely difficult, therefore, to establish relevant metrics and appropriate thresholds to minimize behavioral effects (Southall *et al.*, 2007; Kyhn *et al.*, 2011; Finneran and Jenkins, 2012; Wood *et al.*, 2012; NOAA, 2013; Wisniewska *et al.*, 2014). Behavioral response studies aim to develop dose-behavioral response relationships reflecting the range of sound levels required to elicit a response within a population (e.g., Kastelein *et al.*, 2013a) or the magnitude of response as a function of the stimulus (e.g., Kastelein *et al.*, 2013b). The sound levels that have been reported to start eliciting behavioral responses range between 100 and 180 dB re 1 μPa SPL (Finneran and Jenkins, 2012; Wood *et al.*, 2012; Shannon *et al.*, 2016; Carroll *et al.*, 2017). The SPL depends on the averaging time used, which can lead to a range of possible values for the same pulse depending how the pulse length is determined (Madsen, 2005). It is important to document the variability in the pulse length and SPL with *in situ* data.

Man-made sound has the potential to mask ecologically relevant sounds, especially when the frequency bands of the sound sources overlap. Sounds that are ecologically relevant to marine animals include conspecific calls, predator and prey sounds, natural sounds used for orientation, and echolocation calls from odontocetes (Clark *et al.*, 2009). Seismic airgun arrays emit high-intensity low-frequency sound impulses with peak frequencies of near 50 Hz (Dragoset, 1990; Caldwell and Dragoset, 2000). They are expected to have minimal impacts on marine mammals, such as odontocetes, that have limited hearing sensitivity at these low frequencies (NRC, 2005; Southall *et al.*, 2007; NMFS, 2016). However, Goold and Fish (1998) report frequencies of up to 8 kHz above the ambient background at a distance of 8 km from a 2120 in.^{3} seismic array in 50–100 m deep water, Madsen *et al.* (2006) report measured per-pulse SPLs in the 10 kHz 1/3-octave-band greater than 110 dB at a range of 1.4 km from a 2590 in.^{3} seismic array in deep waters in the Gulf of Mexico, and Hermannsen *et al.* (2015) show energy above 10 kHz from single airguns at a range of 1300 m in 15 m deep water.

In summer 2011, license holders submitted four seismic survey applications to the DCE. As part of the Environmental Impact Assessment process, each proponent's acoustic modeling methods and results (e.g., Matthews, 2012) were reviewed by the DCE, and the cumulative effects of all surveys were assessed. Various data gaps were identified, such as (1) limited documentation of the propagation of seismic airgun pulses around Greenland; (2) limited ambient sound data for Baffin Bay and Melville Bay; (3) limited knowledge of the variation in seismic array sound levels as a function of depth; (4) uncertainty about the importance of high-fidelity inputs for acoustic models (e.g., temperature/salinity profiles, bottom contours, and the sub-bottom geo-acoustic structure); and (5) the temporal and spatial variation of marine mammal distribution in Baffin Bay and Melville Bay (Wisniewska *et al.*, 2014). Comparing measured and modeled sound propagation as a function of depth was noted as especially important, since cold fresh water from melting glaciers creates a strong sound speed minimum at 30–80 m depth, which is expected to trap and propagate low-frequency sounds for long distances in the sound duct.

To address these data gaps, we conducted a multi-year acoustic monitoring program. As part of Shell's seismic survey in the license areas, three vertical array moorings with hydrophones at three measurement depths were deployed in summer 2012 (Fig. 1, also see Sec. II A). We also deployed one bottom-mounted autonomous recorder in Melville Bay from mid-August to mid-September 2012. During August and September 2012, two seismic source vessels conducted a 3-D seismic survey with 3480 in.^{3} airgun arrays near the vertical arrays, including two passes within 110 m slant range of the top hydrophones. The modeled broadside zero-to-peak sound pressure source level of the arrays was 247.3 dB re 1 μPa with a modeled per-pulse sound exposure level of 227.8 dB re 1 μPa^2 s (Matthews, 2012). Five recorders were deployed in September 2013 to study the summer ambient soundscape and to characterize a lower-energy shallow-hazards seismic survey conducted with a 140 in.^{3} array

(modeled broadside zero-to-peak sound pressure source level of the array was 239.3 dB re 1 μPa with a modeled per-pulse sound exposure level of 214.5 dB re 1 μPa^2 s) (Matthews, 2013). Two recorders with hydrophones at mid-water column depth were deployed overwinter from 29 September 2013 to 6 September 2014 to capture the soundscape over a full year (see Sec. II A).

Here we report on the new knowledge derived from the monitoring program through an analysis of the license block and Melville Bay recordings. We present (1) propagation conditions of seismic pulses in Baffin Bay; (2) an overview of ambient sound characteristics, total sound levels, and spectral content associated with seismic pulses in Baffin and Melville Bay; (3) variation in seismic airgun sound levels as a function of depth; (4) a comparison of modeled and measured sound levels at ranges up to 65 km from the source; (5) cumulative sound exposure levels; (6) a comparison of different SPL metrics for predictions of ranges to behavioral disturbance of marine mammals; and (7) the measured spectral content of the pulses as a function of range to the seismic source. Due to the large amounts of data collected in this project, we have provided figures and tables that illustrate points on additional recorder channels in the supplementary material.[1] The data from this project also generated extensive new information on the seasonal presence of marine mammals in Baffin Bay, which is reported in Frouin-Mouy *et al.* (2017).

II. METHODS

This section describes the autonomous recorder deployments and the methods used for analyzing the data and acoustic propagation modeling. With respect to acoustic terminology, this manuscript uses the terms recommended in the final draft of ISO standard 18405:2017. Specifically, sound pressure level is 20 times the base-10 logarithm of the root mean squared pressure summed over a specified time window and is abbreviated as SPL or $L_{\mathrm{p,duration\ rms}}$ where "p" stands for pressure and "duration" is the averaging window length. The maximum of the pressure signal, in dB re 1 μPa, is referred to as peak sound pressure level or $L_{\mathrm{p,pk}}$. The 1/3-octave-band used in this analysis followed the 1/10 decade (deci-decade) definition of 1/3-octaves.

A. Recorders and deployments

Autonomous Multichannel Acoustic Recorders (AMARs, JASCO Applied Sciences) were deployed at Stations BB1–BB4 (Fig. 1, Table S-1)[1] between 29 July and 2 October 2012. Stations BB1–BB3 were bottom-mounted vertical arrays (Fig. 2), with hydrophones at 100, 200, and 400 m water depths. The recording depths were chosen as a compromise between the expected propagation paths (see Sec. II C), water column coverage, and eliminating interference with the seismic arrays. At these three stations, the top hydrophone (100 m depth) sampled continuously at 64 kilosamples per second (ksps) to record seismic airgun pulses and marine mammal calls. The two lower hydrophones (200 and 400 m depth) sampled continuously at 8 ksps, primarily to record seismic airgun pulses. All three hydrophones were sampled by the same AMAR. The 8 ksps sample rate for the lower hydrophones was chosen to maximize the recording duration within the memory capacity of the system (1.792 TB). We chose not to duty cycle these recordings so that the recordings would contain complete overpasses of the seismic vessel at all depths. Station BB3 was located within 3 km of pre-survey modeling Site 3 (Matthews, 2012) to permit comparisons between the measured and modeled data (Fig. 1). At Station BB4, located within Melville Bay, an AMAR was deployed at the seabed (130 m) with a single omnidirectional hydrophone sampling at 64 ksps.

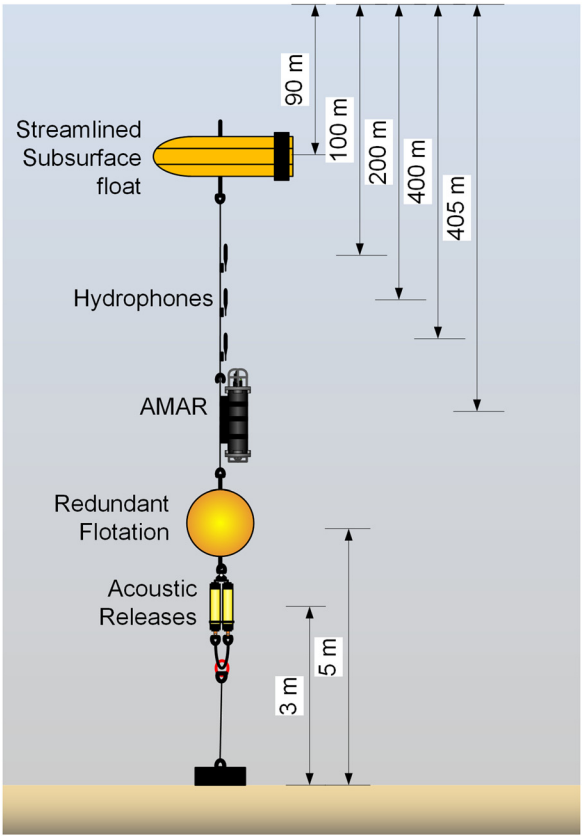

FIG. 2. (Color online) Overview of the mooring configuration used in 2012. The bottom hydrophone was located at ~400 m water depth with the recorder located ~5 m below it. The other hydrophones were located at 200 and 100 m depth. The streamlined sub-surface float was at 90 m depth.

AMARs were deployed at Stations BB5–BB9 (Fig. 1, Table S-1)[1] between 31 August and 30 September 2013. These systems were fitted with GTI-M8E hydrophones which, due to the shorter monitoring period allowed for higher sampling rates, alternated between sampling rates of 64 and 375 ksps. The hydrophones were positioned between 300 and 500 m, in each case near mid-water column for the chosen locations (Table S-1).[1] To collect a year-long dataset without seismic activity, AMARs were deployed at Stations BB6 and BB10 from late September 2013 to early September 2014 (Fig. 1, Table S-1).[1] Each year-long AMAR was fitted with a GTI-M8E-V35 dB omnidirectional hydrophone and cycled between 64 and 375 ksps, as well as periods of sleep. The details of hydrophone sampling configurations and sensitivities are given in Tables S-2[1] and S-3.[1]

B. Acoustic data analysis

Acoustic data were quantified using three standard metrics: peak sound pressure level, sound exposure level (SEL), and sound pressure level (SPL) (see, for example, Madsen, 2005 for definitions of these metrics). The broadband SPL, as well as the SPL, in each 1/3-octave-band were computed. The metrics were computed for each minute of data to characterize the total sound levels and separately for each detected seismic pulse to characterize the short impulses. The one-minute deci-decade SPLs were converted to deci-decade SELs by adding 10*log10(60 s) and combined to assess the frequency-weighted sound levels (Southall *et al.*, 2007) or to compute the sound levels in octave bands so seismic sound levels could be discussed as a function of frequency. The 1 Hz power spectral densities averaged over 1 min were computed and are presented in the Sec. III A and the supplementary material[1] as long term spectrograms, percentile levels, and spectral probability densities (see Merchant *et al.*, 2015 for a discussion of these methods).

Our analysis used exceedance percentile levels to quantify the distribution of recorded sound levels. Following standard acoustical terminology, the *n*th percentile level (L_n) is the level (i.e., power spectral density level, SPL, or SEL) exceeded by *n*% of the data. L_{max} is the maximum recorded sound level. L_{mean} is the linear arithmetic mean of the sound power, which can differ significantly from the median sound level L_{50}. The exceedance percentiles are often presented as statistical sound levels using box- and-whisker plots (e.g., Fig. 5). In such plots, the bottom and top of the "box" are defined by the 75th and 25th percentile sound levels, respectively, and a line through the middle of the box shows the median level. Whisker lines extending above and below the box show the total range of measured data, with short hash marks to indicate the 95th and 5th percentiles. The mean (L_{mean}) value is shown with a separate line across the plot.

Seismic survey pulses were identified using a variation on the Teager-Kaiser (TK) energy detector (Kaiser, 1990). The detector created an "energy" time-series as the square root of the sum of the squared pressure signal over a period of 0.03 s. A detection was determined to have occurred when the square of this time series (sample X_i) was greater than the product of its neighbors by a chosen threshold [Eq. (1)]:

$$X_i^2 - X_{i-1} * X_{i+1} > T. \quad (1)$$

The pulse limits were defined by searching for the maximum energy in the neighborhood of each detection. Two versions of the detector were implemented for this study. The first version used the 90% energy duration method of analyzing man-made impulsive sounds (T90 SPL, e.g., Blackwell *et al.*, 2004; Thode *et al.*, 2010) by searching over a 7 s window and finding the period that contained 90% of the energy (7 s was required due to the extensive multi-path arrivals, see Fig. 7 and Fig. 8). The second version limited the duration of the impulse to the integration time of mammalian hearing (Madsen, 2005; Tougaard *et al.*, 2015) by searching over a 0.5 s time window centered on the TK-detection and finding the 0.125 s period with the maximum energy. Multi-path arrivals from a single airgun pulse were separated into distinct impulses for analysis when we used the second approach. We chose the 0.125 s window based on Tougaard *et al.* (2015) because it is also the standard used in terrestrial sound level meters for fast-time weighting (ANSI S1.4-1983, 2006) and hence will be simpler for other teams to replicate in the future. The results of these two approaches were compared with the total 1 min sound levels computed from the same time periods.

The data were pre-conditioned using a 10 Hz high-pass digital filter to remove very low-frequency electrical noise caused by an improper power supply to the current-loop circuits of the hydrophones. The finite impulse response filter was designed with the MATLAB (The Mathworks Inc, Natick, MA) *Filter and Window Design Application*, with a 7 Hz stop frequency, a 10 Hz pass frequency, and 60 dB of stop-band attenuation using the "Kaiser Window" design option. The filter had 77342 points, and it did not significantly affect the measured signal levels above 10 Hz. Analysis of seismic pulses received 40 km from the source before the electrical noise began (5–6 August) showed up to a 0.2 dB difference in the per-pulse SPL and SEL, and up to a 1.5 dB difference in the peak sound pressure level. Processing of the wav file recordings was performed using the PAMlab software suite (JASCO Applied Sciences). Post processing of the PAMlab outputs and plot generation was performed using custom MATLAB scripts.

C. Seismic source and acoustic propagation modeling

Acoustic propagation modeling was a four-part process: (1) modeling of the airgun source; (2) modeling per-pulse sound exposure level propagation loss using a range-dependent parabolic equation model, (3) combining the source level and propagation loss to estimate the per-pulse SEL at the water volume around the source, and (4) converting the per-pulse SEL to SPL. The first two steps were performed at individual deci-decade center frequencies between 10 and 2000 Hz, and the contributions of each band were summed during the final step. We used the Airgun Array Source Model (AASM, JASCO Applied Sciences) to estimate the source signature of each airgun in the array by simulating the physics of bubble expansion and interactions with adjacent bubbles. The frequency dependent source level and beam pattern of the array were estimated by convolving the signatures of the individual airguns taking into account the geometry of the array (MacGillivray, 2006; Matthews, 2012). The Marine Operations Noise Model (MONM, JASCO Applied Sciences) was used to perform parabolic equation propagation loss modeling. MONM is based on the U.S. Navy's Range-dependent Acoustic Model (Collins, 1993), modified to use complex density to approximate shear wave conversion energy loss at the seafloor (MacGillivray, 2006; Matthews, 2012; MacGillivray, 2013).

Propagation loss estimates are affected by the bathymetry, water column sound speed profile, and acoustic properties of the seabed. Pre-survey modeling (Matthews, 2012) was performed using sound speed profiles from the Generalized Digital Environmental Model (GDEM) database

(Teague *et al.*, 1990), bathymetry from the SRTM 30 data set (Rodriguez *et al.*, 2005), and a five-layer seabed geoacoustic profile based on available literature (Table S-4).[1] The sound speed profile in this area has a strong sound speed minimum at ~60 m depth because of cold fresher water lying over warmer more saline water (e.g., Fig. S-3).[1] Therefore, we expected that sound would refract towards the sound speed minimum and that there would be higher sound levels at 100 m recording depth compared to the lower recording depths (see Sabra *et al.*, 2016 for an introduction to long range underwater sound propagation). Due to the width of the measured sound duct (~15 m/s change from 30 to 100 m depth) the measured sound levels at higher frequencies may slightly less than could have been measured at 60 m at long ranges.

Per-pulse SELs were converted to T_{90} SPLs using a range dependent estimate of the pulse length. The pulse length was estimated by generating a synthetic pressure waveform for the airgun array through a Fourier synthesis of the waveform. The vertically and azimuthally directional starting field for the sound propagation model was generated in a 1-Hz frequency bin from 10 to 2000 Hz, based on the source signature computed by AASM and the relative position of each array element. The propagated sound field was summed across frequency, and then an inverse Fourier transform was performed to obtain the modeled waveform. The pulse length was obtained from the modeled waveform to produce a per-pulse SEL to SPL conversion factor. During the pre-survey modeling, two conversion factors were estimated, one eastward from Station BB1 and the other westward from BB1. For the post-survey analysis, a conversion factor along bearing of 030° (northeast) from Station BB1, towards BB3, was computed.

During data analysis, the measured and modeled sound levels were compared. Further modeling was performed to investigate if the differences between the measured and modeled sound levels could be reduced by increasing the frequency resolution of the modeling, running the model with the measured sound speed profiles, or using the bathymetry measured by the seismic vessels.

D. Greenland seismic surveys in 2012 and 2013

Seismic surveys were conducted in the Shell-operated license areas in 2012 and 2013. The 2012 3-D survey was conducted by the *Polarcus Amani* and *Polarcus Samur* from 2 August 2012 to 15 October 2012. In that year, each vessel towed two 3480 $in.^3$ seismic arrays (Fig. S-2).[1] The arrays on each ship were operated alternately so that the average sounding rate per ship was 10–12 s. The median survey speed was 2.25 m/s, or 8.1 km/h. The vessels operated independently throughout the survey. The ships occasionally operated in the same area on parallel acquisition lines, separated in time by a 4 h delay (32 km separation). Approximately 228 000 pulses from the *Amani* and 220 000 from the *Samur* were recorded. The median ranges of the *Amani* to Stations BB1, BB3, and BB4 were 42, 106, and 124 km, respectively (Table I, Fig. 3). The median ranges to the *Samur* were 36, 62, and 105 km, respectively. The vessel tracks that passed closest to Station BB1 on 4 September 2012 and BB3 on 18 September 2012 are examined. Station BB2 measurements were similar to BB1, so only BB1 is analyzed in detail.

TABLE I. Minimum, median, and maximum distances from the *Amani* and *Samur* to Stations BB1, BB3, and BB4 (Fig. 1) in summer 2012.

Ranges from survey vessel to station	Minimum distance (km)	Median distance (km)	Maximum distance (km)	Median daily closest point of approach (km)
Amani to:				
BB1	0.1	42	89	16
BB3	0.02	106	153	40
BB4	68	124	158	95
Samur to:				
BB1	0.7	36	90	14
BB3	0.6	62	153	25
BB4	68	105	158	95

Two other seismic surveys occurred in summer 2012 in Baffin Bay. ConocoPhillips, DONG Energy, and Nunaoil jointly conducted a 2-D survey from 25 August 2012 to 24 September 2012 in the license area north of the Shell license area. This survey's closest point of approach was ~40 km to Station BB3 and 120 km to BB4. Maersk Oil conducted a

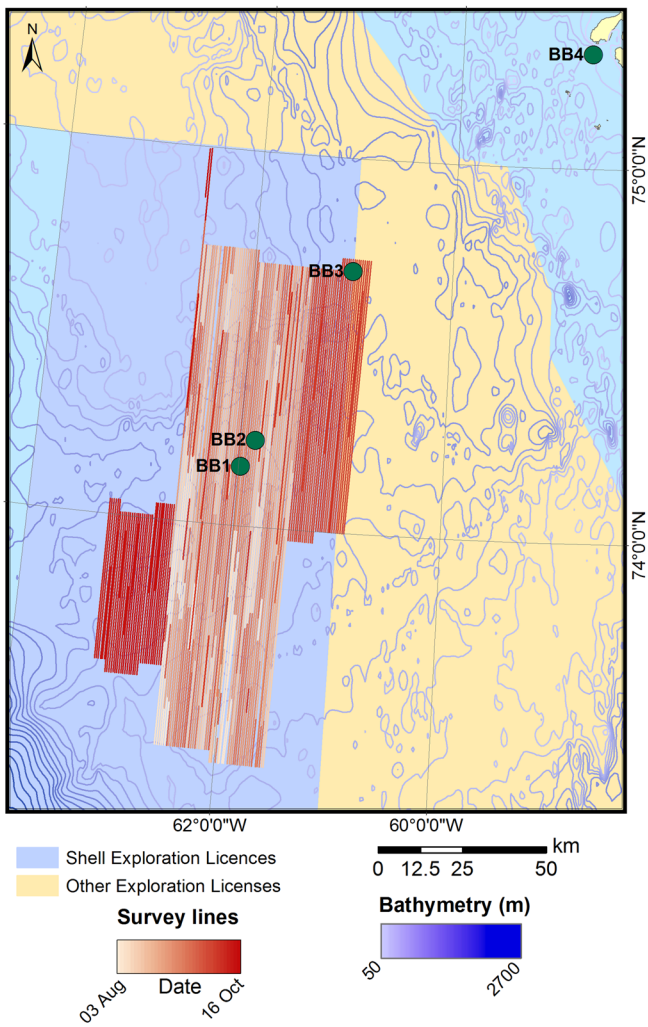

FIG. 3. (Color online) Survey lines of the *Amani* and *Samur* in summer 2012.

3-D survey from 6 August 2012 to 1 October 2012 in the license area southeast of the Shell license area. This survey's closest point of approach was 100 km to Station BB1 and at least 200 km from BB4 (Wisniewska *et al.*, 2014).

From 15 September 2013 to 8 October 2013 the *Fugro Discovery* conducted a localized shallow-hazards survey for Shell Oil by using a 140 $in.^3$ array (Table S-5,[1] Figure S-1).[1] Shallow hazards surveys detect features that may impact proposed oil and gas operations such as gas vents, abnormal pressure zones, and faults lines. Here we present the data from Station BB6 as an example of measurements that were 40 or more kilometers from the shallow-hazards survey, and BB7 as an example of recordings within the region of the survey. The two summer data sets with seismic surveys are compared with the year-long data from Stations BB6 and BB10.

III. RESULTS AND DISCUSSION

A. Soundscapes of Baffin and Melville Bays

The various sets of acoustic data acquired during this project are characterized by different combinations of man-made and natural sounds (Fig. 4): (1) the year-round recording at Station BB6 shows minimal man-made sounds; (2) the September 2013 recording at BB7 reveal few man-made sources until the start of the shallow hazards survey on 15 September 2013; (3) the nearshore recordings in Melville Bay (BB4) from 2012 are dominated by glacial ice sounds; and (4) the BB1 recordings from 2012 prominently feature the 3-D seismic survey. When the seismic surveys started on 2 August 2012 and 15 September 2013, the average sound levels near the operations increased. The average 1-min SPL at Station BB1 was 106 dB re 1 μPa prior to 2 August 2012 and 134 dB re 1 μPa after that date, with most of the increase at frequencies below 100 Hz (Fig. 4, Panel 4). The received sound levels at that station increased and decreased as the survey vessel approached and departed. Other stations (e.g., Station BB3, Fig. S-4)[1] had similar results. The sounds from the surveys in the other license areas are not discernible in these figures.

The summer 2012 stations were deployed 29 and 30 July 2012 and retrieved 29 September 2012 to 2 October 2012 (Table S-1).[1] Since the seismic survey started on 2 August 2012, there were little data available from 2012 to

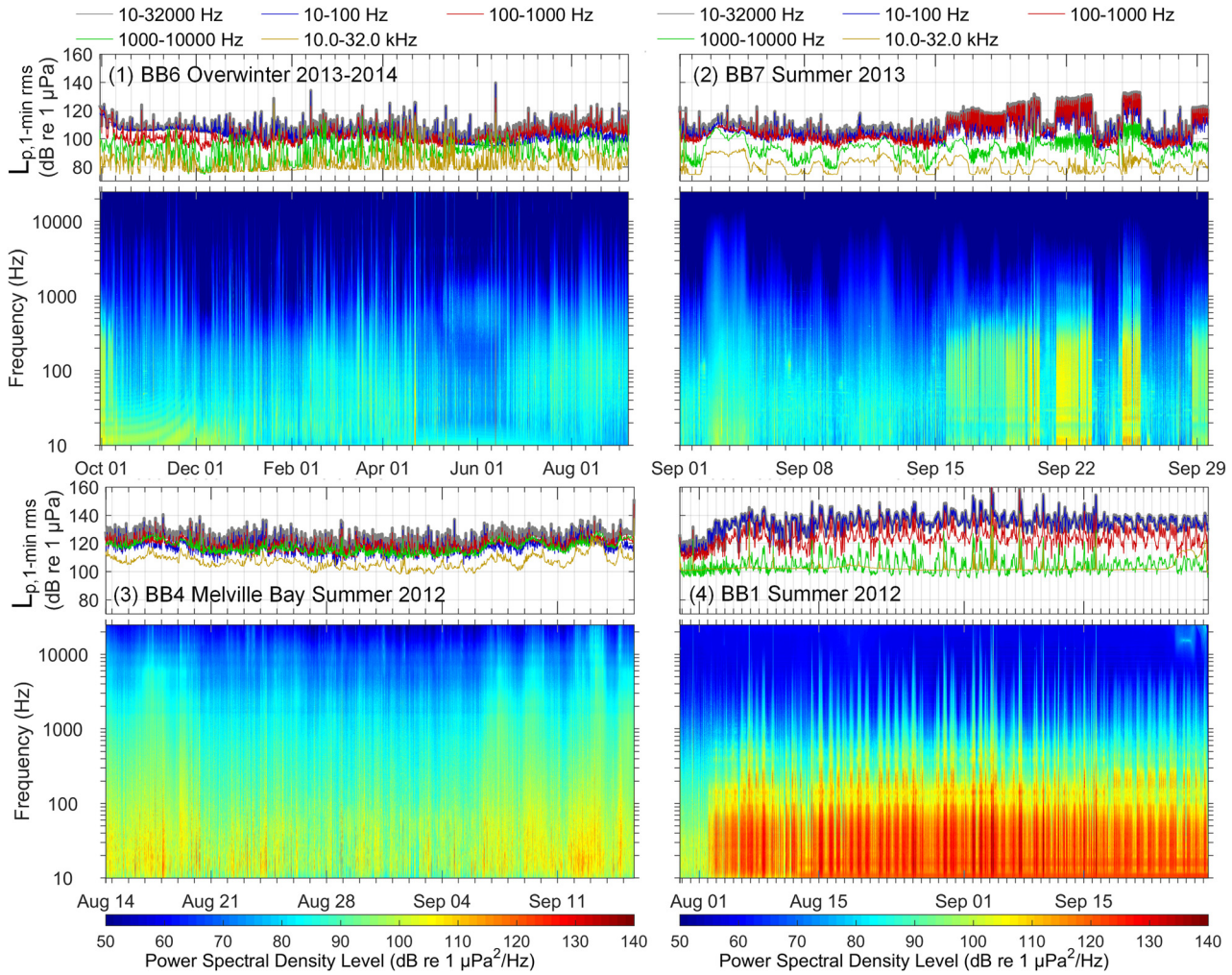

FIG. 4. (Color online) Summary of the received sound levels in Baffin Bay for four sound scenarios: (1) Station BB6 in overwinter 2013–2014 with minimal man-made sounds; (2) BB7 in summer 2013 at 3–100 km from a shallow hazards survey that started 15 Sep; (3) BB4 near glacial ice in Melville Bay in 2012; and (4) BB1 in summer 2012 at 0.1–90 km from the 3-D seismic survey that started 2 Aug. The bottom section of each figure shows long-term spectrograms and the top section corresponding band-level time-series plots.

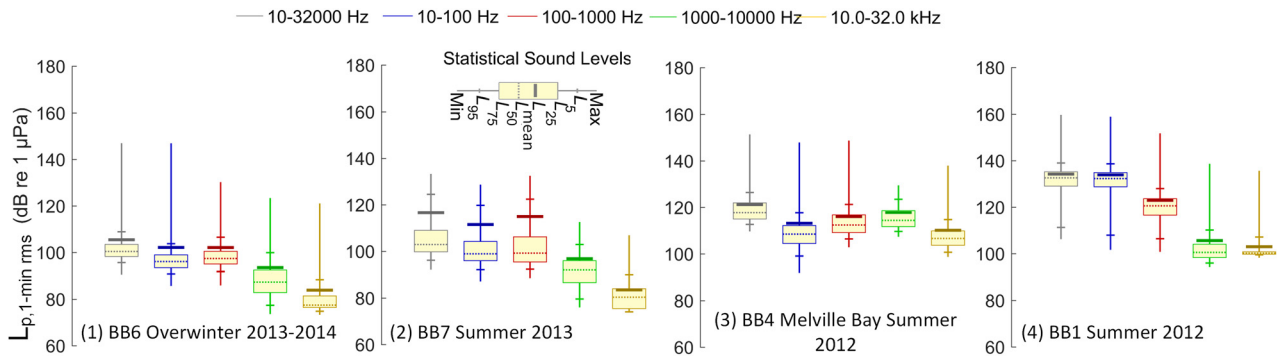

FIG. 5. (Color online) Comparison of the statistical received sound levels for the four sound scenarios in Fig. 4. From left to right the bands are 10–32 000, 10–100, 100–1000, 1000–10 000, and 10 000–32 000 Hz.

assess the natural ambient soundscape in Baffin Bay. The summer 2013 and overwinter 2013–2014 recordings provide data for this purpose (Fig. 5, Fig. S-4,[1] Fig. S-6,[1] Fig. S-8[1]). Figure 5 shows the distribution of 1-min SPLs in four of these recordings. Broadband (10–32 000 Hz) and four decade bands are shown. The 10–100 Hz band normally contains sounds from natural and anthropogenic seismic sources, calls from the very large baleen whales, as well as possible pseudo-noise from flow over hydrophones and cable strum. Large vessels, seismic surveys, baleen whales, and wind and wave action are the primary sources of sound in the 100–1000 Hz band. The 1000–10000 Hz band contains sounds from wind and wave action and potentially whistles from pilot whales and narwhals. The 10 000–32 000 Hz band normally contains energy from whistles, echolocation clicks, and rain (see Cato, 2008; Hildebrand, 2009 for summaries of ocean noise).

Station BB6 is representative of ambient sound level measurements in Baffin Bay with a median SPL of 102 dB re 1 μPa in summer 2013 and 100 dB re 1 μPa overwinter 2013–2014 (Figs. 5, S-6,[1] and S-8[1]). There were few anthropogenic sound sources in this period, and no 3-D seismic surveys were conducted. The general shape of the spectra are similar to those reported from sonobuoy studies in 1981 (Leggat *et al.*, 1981). The 100–1000 Hz band, driven by wind action, has the highest sound levels during summer. During winter, ice cover reduced the sound levels above 100 Hz from December to May (Figs. S-61 and S-8[1]) (see also Roth *et al.*, 2012). Biologic sound sources were infrequent, with the exception of bearded seals (*Erignathus barbatus*) in May and June (Frouin-Mouy *et al.*, 2015).

The sound spectra recorded at Station BB4 in Melville Bay were consistent with glacial ice melt. The median 1-min SPL was 116 dB re 1 μPa, 14 dB higher than the 102 dB re 1 μPa at Station BB7 in summer 2013 (Figs. 5, S-5,[1] and S-8[1]). The highest Melville Bay sound levels were in the 1000–10 000 band, whereas in the data from other stations the 1000–10 000 Hz band were much lower than the 100–1000 Hz and 10–100 Hz bands. Listening to the sound files from Station BB4 (e.g., the data represented in Fig. S-7)[1] reveals many instances of ice cracking, as well as pops and hisses that are likely caused by air escaping from melting glacial ice (Pettit *et al.*, 2015). This is reasonable given that station is near the Greenland coast and its calving glaciers (Fig. 1).

Seismic pulses were rarely detectable at Station BB4 (e.g., Fig. 4), and the 1-min SPL was uncorrelated with the distance to the *Samur* and *Amani* (Fig. 6, $r^2 = 0.017$, SE = 0.31). The periods with higher sound levels (e.g., 7–13 September 2012, Fig. 4) did not contain pulses originating from the seismic surveys in the adjacent lease areas either; instead, these periods contained more loud ice cracking events than the quieter periods.

The octave-band 1-min SPLs at Station BB6 in September 2013 (Fig. S-8,[1] Table S-5[1]) were used to establish a threshold where the seismic survey sounds would stand out against the ambient background sounds and begin masking other sounds in the same band as the received seismic energy (see Sec. III G). The data preceding the 2012 seismic survey were not used because the time period was quite short and the dynamic range of the 2012 ambient recordings was limited by the low sensitivity of the M8E-0 dB hydrophones (see Table S-3).[1]

B. Nature of seismic airgun pulses in Baffin Bay

The seismic pulses recorded in Baffin Bay showed very strong multipath arrivals for source-recorder ranges (or separations) of less than 40 km (Figs. 7 and 8). The pattern of arrivals depended on the depth of the hydrophone, the water depth (770 m), and the range to the seismic vessel. At 100 m hydrophone depth (Fig. 7), the pulses arrived in pairs, where the first one was the upward traveling reflection from the seabed and the second was the downward traveling surface reflection. As the range to the vessel increased, the time between the impulses in each pair decreased due to the

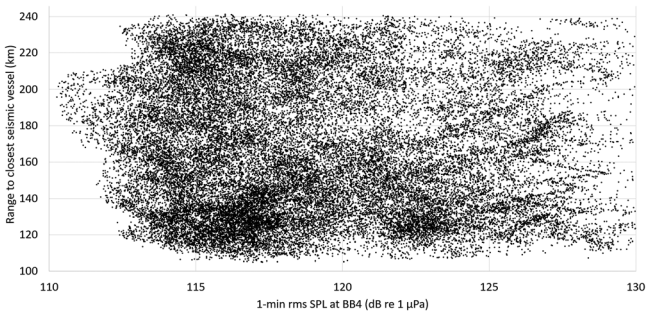

FIG. 6. Ranges from Station BB4 to the *Samur* and *Amani* in summer 2012 and the 1-min SPL.

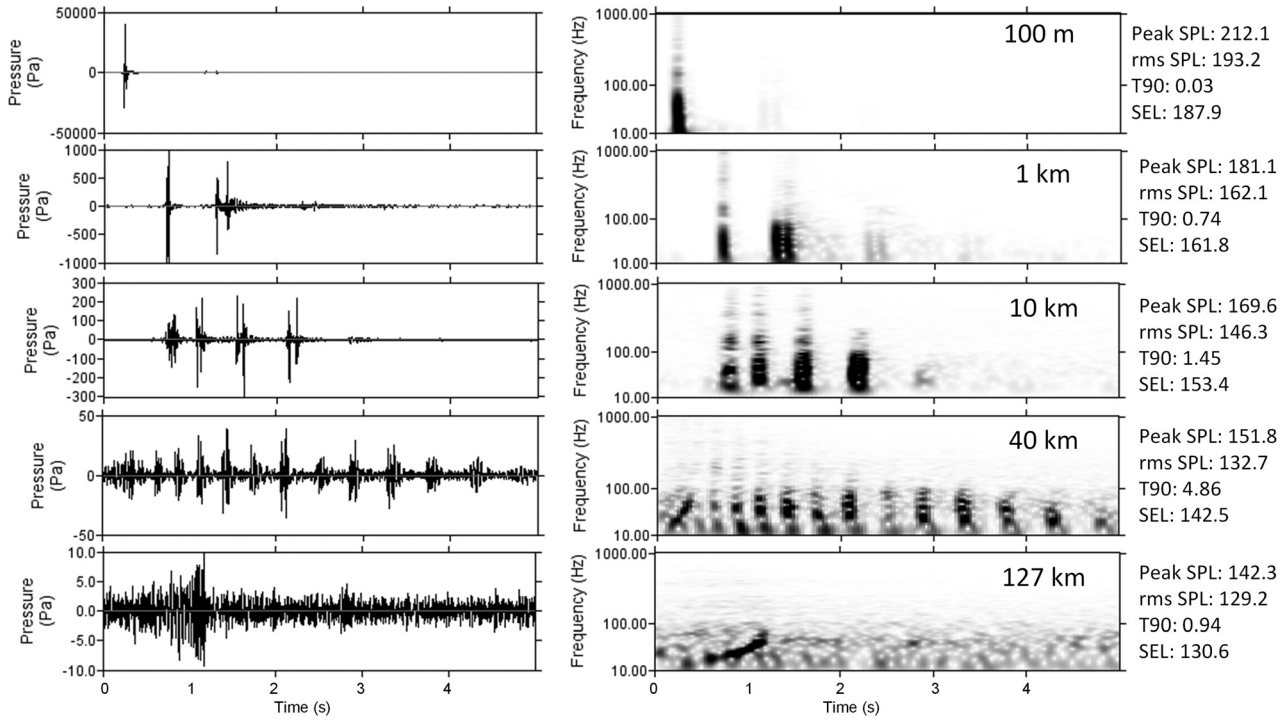

FIG. 7. Shape of 3480 in.^{3} seismic array pulses at progressively longer ranges from Station BB3 in 770 m water depth at the 100 m deep hydrophone. All figures show 5 s of data. (Left) Time-series waveforms, and (right) spectrograms (1 Hz resolution, 0.2 s of data per FFT, 0.19 s overlap between FFTs, Hamming window). The SPL and SEL are for the T_{90} window durations shown.

reduced differences in path length. The number of pairs arriving at the hydrophone also increased with range. At the 400 m hydrophone (Fig. 8), the path lengths between the bottom and surface reflections were the same; hence, the impulses were evenly spaced. Similar to the measurements at 100 m water depth, the number of impulses increased with the distance to the vessel. The additional impulses increased the 90% energy duration every time an additional propagation path became important (Fig. 9). The duration decreased with range as the length of the propagation path shortened. At ~40 km from the source, the number of arrivals depended on many propagation variables (e.g., bathymetry, bottom

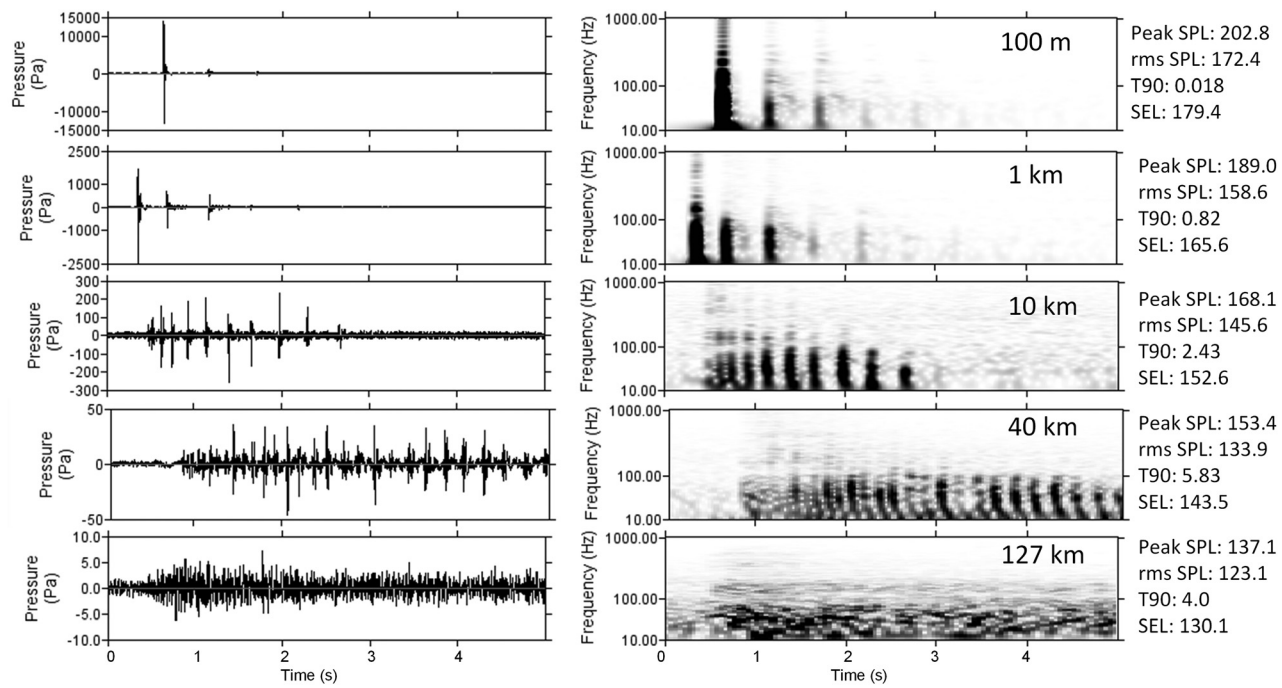

FIG. 8. Shape of 3480 in.^{3} seismic array pulses at progressively longer ranges from Station BB3 in 770 m water depth at the 400 m deep hydrophone. These are the same pulses as shown in Fig. 3 at 100 m depth. All figures show 5 s of data. (Left) Time-series waveforms, and (right) spectrograms (1 Hz resolution, 0.2 s of data per FFT, 0.19 s overlap between FFTs, Hamming window). The SPL and SEL are for the T_{90} window durations shown.

scattering roughness, weather), and the pulse lengths ranged from 2 to 6 s (Fig. 9).

Also at ~40 km from the source, the received signal at 100 m depth began to exhibit a frequency upsweep pattern in the 0.5–1 s initial arrival in the time series. This pattern became the dominant spectral feature at ranges greater than 40 km. These sweeps were the result of the sound being refracted into a low-velocity sound channel (Fig. S-3).[1] Higher frequencies were refracted more steeply than the lower frequencies, resulting in a longer path length and thus later arrivals at higher frequencies. Upsweeps were faintly present at 200 m depth, but they were not detected at 400 m depth (Fig. 8).

The pulses recorded in Baffin Bay had a different character than those reported from other deep water measurements, in that the direct arrival and subsequent multipath arrivals in the recordings from Baffin Bay study had similar amplitudes (within 1–6 dB). These signal characteristics were sustained at ranges between 1 and 40 km, unlike those reported by Madsen *et al.* (2006) from deep waters in the Gulf of Mexico where the first arrival had much higher levels than the multipath arrivals. The pulse structure was also different than the long reverberant pulses observed at intermediate ranges in deep water in the Lau Basin by Bohnenstiehl *et al.* (2012b); however, the long range pulses (127 km) recorded at 400 m depth in Baffin Bay were similar to the Lau Basin pulses at comparable ranges (Fig. 8).

The presence of many multipath arrivals in the present data suggests a smooth and flat seabed with a high reflection coefficient in the Baffin Bay project area. The Lau Basin region, by comparison, is a tectonic spreading zone with a very high sound speed bottom (primarily basalt with little surface sediment accumulation) that should be an excellent reflector. However, random seafloor deformations at the Lau Basin spreading zone scatter the higher frequencies so that only low frequencies propagate long distances in the Lau Basin Bay. We note, by contrast to the deep water propagation conditions in Baffin Bay and the Lau Basin, that seismic pulses received in shallow water areas (<100 m) are affected by shallow water filtering (Urick, 1983), head waves from higher speed propagation in the substrate, and modal dispersion (Guerra *et al.*, 2011; Guan *et al.*, 2015).

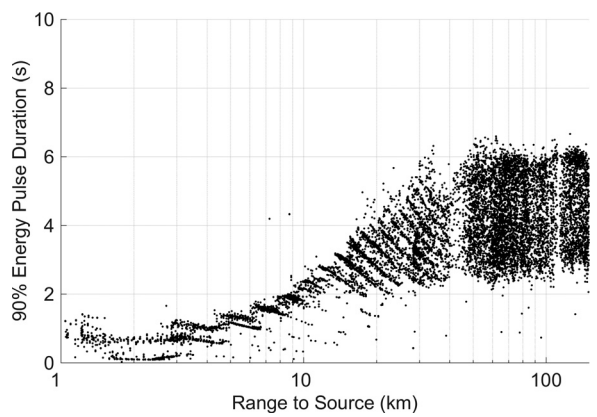

FIG. 9. The 90% energy pulse duration compared to range for the data received at Station BB1 and BB3's 100 m deep hydrophones. Data were selected from 3.7 days when only a single seismic vessel was active. Ranges to the vessels were 1–150 km. For each minute of seismic activity, the five pulses with the highest energy were selected and plotted.

C. Cumulative sound exposure and predictions of ranges to radii for auditory injury of marine mammals

As discussed in the Introduction, recent frameworks for assessing the effects of noise on marine life (e.g., Southall *et al.*, 2007; Popper *et al.*, 2014; NMFS, 2016) use two criteria to assess the risk of auditory injury: peak sound pressure level and cumulative SEL. For airgun arrays, the peak sound pressure level drops below the injury threshold level for marine mammals at a range of tens of meters. The cumulative SEL drops below the suggested regulatory sound levels for injury at ranges of hundreds of meters and can be 1 km or longer and becomes the zone that is monitored for protection of marine mammals (e.g., Matthews, 2012). This is especially true for a stationary receptor. Thus, an analysis of the cumulative SEL metric using the Greenland data may be instructive for future regulatory discussions.

The radius around the source where the measurements suggest possible auditory injury to marine mammals depends on which set of thresholds and auditory weighting functions are used. The *Guidelines to Environmental Impact Assessment of Seismic Activities in Greenland Waters* (Kyhn *et al.*, 2011) mandates the M-weightings and thresholds recommended in Southall *et al.* (2007). In the intervening period between the project and present, new approaches have been distributed by the National Ocean and Atmosphere Administration (NOAA) for the United States. Each approach uses different auditory weighting methods and thresholds for auditory injury and behavioral disturbance. To estimate the ranges when the cumulative SEL exceeded the thresholds, we computed the frequency-weighted daily SEL at Stations BB1 and BB3 and plotted them against the closest point of approach of the seismic vessels for that day (Fig. 10). The Southall *et al.* (2007) weighting functions and thresholds predict potential hearing damage for pinnipeds at ranges of 600 m from the vessel and that low-frequency cetaceans could be injured at very close ranges (<100 m, Fig. 10). The NOAA Technical Guidance (NMFS, 2016) weighting functions and thresholds predict that the acoustic energy from this survey could injure high-frequency cetaceans at ranges of less than 500 m (Fig. 10). On eight days when the seismic vessels' closest points of approach to the stations were greater than 10 km, the measured exposure levels were exceeded the high-frequency cetacean threshold. Our review of these events showed that seismic sounds were present; however, additional energy from the close passage of other vessels (ranges and vessel identities are unknown) increased the sound levels in the high-frequency weighted cetacean SEL for those days. The NOAA Technical Guidance threshold for exposure of high-frequency cetaceans to non-impulsive sounds is 173 dB re 1 μPa^2 s, and these exposures do not exceed the threshold. The data were included as "seismic" by the automated processing since detection was performed on unweighted data and the weighting applied to the impulses after detection. These results highlight the continued need for research into the appropriate auditory

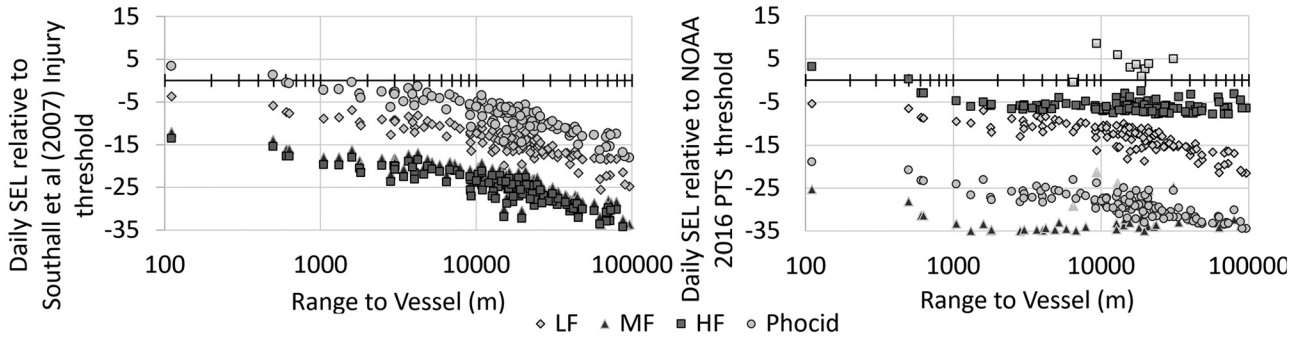

FIG. 10. Exceedance of frequency-weighted daily SELs compared to three injury metrics versus the closest range to either seismic vessel for the 100 m hydrophone at Station BB1. (Left) Southall *et al.* (2007) injury threshold. (Right) NOAA Technical Guidance (2016) permanent threshold shift (PTS). Positive values exceed the thresholds. Frequency band abbreviations: LF—low-frequency cetacean auditory weighting; MF—medium-frequency cetacean auditory weighting; HF—high-frequency cetacean auditory weighting; Pinniped—pinniped weighting from Southall *et al.* (2007) and the phocid weighting from NOAA Technical Guidance (2016). The light-gray shaded high-frequency data also contained significant levels of energy from the close passage of vessel and hence are comparable to the threshold of 173 dB re 1 μPa^2 s rather than 155 dB re 1 μPa^2 s, and hence do not constitute an exceedance of the thresholds.

weighting functions for marine species, the effects of sound on marine life, methods of data analysis, and thresholds that will minimize impacts.

D. Depth dependence of seismic pulse energy

DCE's review of the possible effects of seismic surveys on marine life raised the question of variation in the received levels as a function of depth (Wisniewska *et al.*, 2014); therefore, our study recorded acoustic signals at 100, 200, and 400 m below the sea surface. We found that the SPL, per-pulse SEL, and 24-h SEL showed only minor variations in the received sound levels as a function of depth in Baffin Bay. Figures 7 and 8 show that the received sounds at ranges beyond 40 km from the source at a 100 m depth contained a low-frequency upsweep that was not present at 200 and 400 m depth, as described in the Sec. III B. In the longest-range case (127 km), the SPL at 100 m depth was 6 dB higher than at 400 m; however, the pulse was also four times shorter at 100 m, which resulted in the same SEL at both depths.

At close ranges (0–3 km) there were differences with depth in the received signals that depended on the multipath reflections arriving at different times and the vertical beam pattern of the seismic array (Fig. 11). Because the hydrophones were at different depths, the first reflection of the seismic pulse arrived at the 400 m hydrophone, followed by the 200 m and finally the 100 m hydrophone. This pattern was reversed for the subsequent surface reflection (Fig. 11). Seismic arrays concentrate sound in the vertical direction with an angular beam width that depends on frequency (Fig. S-9).[1] As the vessel approached within 1 km of the recording station, the deepest hydrophone "entered" the beam first, and therefore as the vessel approached the received sound level at 400 m depth rose before the levels at the 200 and 100 m depths (Fig. 11). At the closest point of approach, all three hydrophones were almost entirely in the main lobe of the seismic array, so that the 100 m deep hydrophone had the highest sound levels since it was closest to the array and had the lowest geometric spreading loss.

The daily SEL integrates the received exposure levels over a 24-h period and provides a macroscopic assessment of the sound levels as a function of depth. The SELs were virtually identical at all depths, except when the source passed directly over the receivers. The single pulse SELs at the closest point of approach differed by 7 dB between the 100 and 400 m recordings (Fig. 11), yet the daily SELs only differed by 2 dB (Fig. 12). The frequency content at all depths was also virtually identical (not shown). We conclude that for the purposes of assessing the possibility of auditory injury or behavioral disturbance to marine mammals, the sound levels as a function of depth can be treated as uniform for the conditions in Baffin Bay.

E. Verification of propagation modeling results with actual environmental inputs

A knowledge gap identified during the pre-survey modeling effort (Wisniewska *et al.*, 2014) was the poor understanding of the dependence of acoustic propagation model results on the accuracy of the environmental inputs, since there was little high fidelity data available for Baffin Bay to base such an analysis on. The acoustic measurements collected as the seismic surveys passed Stations BB1 and

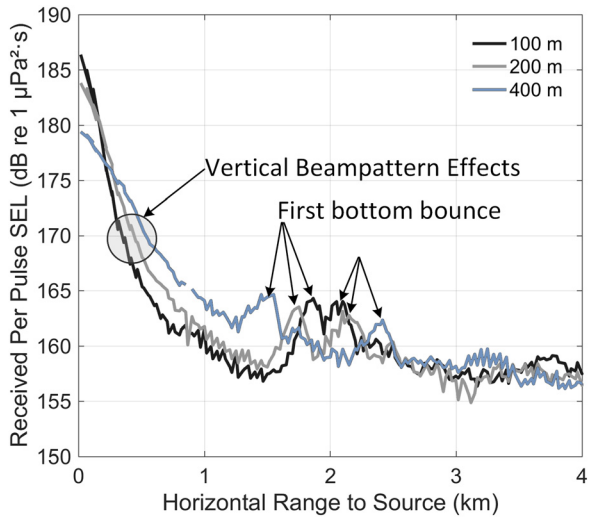

FIG. 11. (Color online) Per-pulse SEL for 125 ms impulses detected at Station BB3 hydrophones from the 3480 in.^{3} seismic source as it passed the station on 18 September 2012. Differences in received sound levels were primarily within the first 3 km from the source.

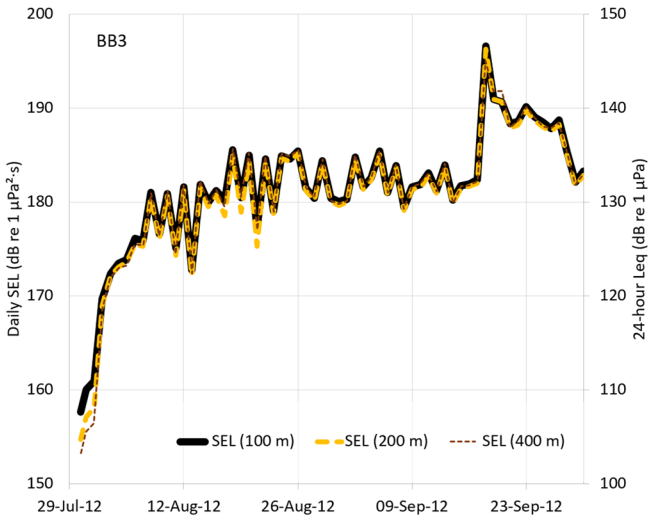

FIG. 12. (Color online) Daily SEL at Station BB3 for the entire recording period at each hydrophone depth. Differences in SEL between depths were only measured before the seismic program started and when the source passed directly over the receivers. Stations BB1 and BB2 produced similar results.

BB3 enable us to directly compare the environmental parameters used for the pre-survey acoustic modeling (Matthews, 2012). The acoustic propagation model was re-run with the source at the vessel's closest point of approach to Station BB1 along the radial from BB1 to BB2 and BB3 (Fig. 1). The measured per-pulse fixed window SPL as the ship approached Station BB1, as well as the simultaneous measurements at BB2 and BB3, were compared to the pre- and post-survey modeled SPLs. The SPLs were computed by applying a range-dependent conversion factor to the SELs modeled by MONM. The conversion factor was computed by running a full waveform version of MONM and computing the pulse duration as a function of range. The pre-survey modeled levels were 3–7 dB higher than the measured values at ranges greater than 500 m (Fig. 13, left). Using the measured sound speed profile did not improve the error significantly. The results were improved (Fig. 13, right) by improving the correction factor. The full waveform model was re-run using the bathymetry measured by the seismic survey vessels along the line from Stations BB1 to BB3 and the measured sound speed profile (Figs. S-10[1] and S-3[1]). The pre-season conversion factor had been computed along two radials, one from Station BB1 east and the other west. By using the more accurate conversion factor, the error reduced to 0–4 dB, even 65 km from the source.

F. Approaches for computing SPL

The first regulatory guidance for limiting effects of sound on marine mammals used the per-pulse SPL as the threshold metric for both behavioral disturbance and injury. Subsequent research has concluded that dual thresholds for the peak sound pressure level and weighted sound exposure levels are appropriate for limiting injury from sound (Southall *et al.*, 2007; Popper *et al.*, 2014; NMFS, 2016), however no direction has emerged for behavioral disturbance. Madsen (2005) clearly articulates the issues with variable length windows when calculating an impulsive SPL. Here we provide results from the long-term and long-range Baffin Bay dataset that supports Madsen's assertion. We demonstrate that if SPL must be used, any fixed window duration is preferable to a variable length window (e.g., the 90% energy duration). We then show how this result supports Tougaard *et al.* (2015) argument that it is essential that the metric used to establish a regulatory threshold be the same one that is used to measure compliance.

Measuring the peak and average sound levels is inherent in any study of the response of marine life to sound stimuli. In addition to the behavioral state of animals, the wide variability within and between the responses of individual animals makes it difficult to understand what elements of the sound are eliciting a response. It may be the similarity of a sound to predator calls, frequency content, absolute level, duration, the onset of the sound, rise time, perceived distance to the source, perceived motion of the source, or other cues not yet discovered (Wartzok *et al.*, 2003; see reviews in NRC, 2005; Nowacek *et al.*, 2007; Southall *et al.*, 2007; Gedamke *et al.*, 2011; Ellison *et al.*, 2012; Pirotta *et al.*, 2012; Risch *et al.*, 2012; Deruiter *et al.*, 2013; Goldbogen *et al.*, 2013; Popper *et al.*, 2014; Miller *et al.*, 2015). Early studies of the effects of impulsive sound on marine life measured the SPL over a time window that includes 90% of the pulse energy (Blackwell *et al.*, 2004; Thode *et al.*, 2010). Madsen (2005) and Madsen *et al.* (2006) advocate computing the SPL over a maximum window of 100–200 ms, the presumed integration time range of the hearing system for most mammals, including all marine mammals that have been tested.

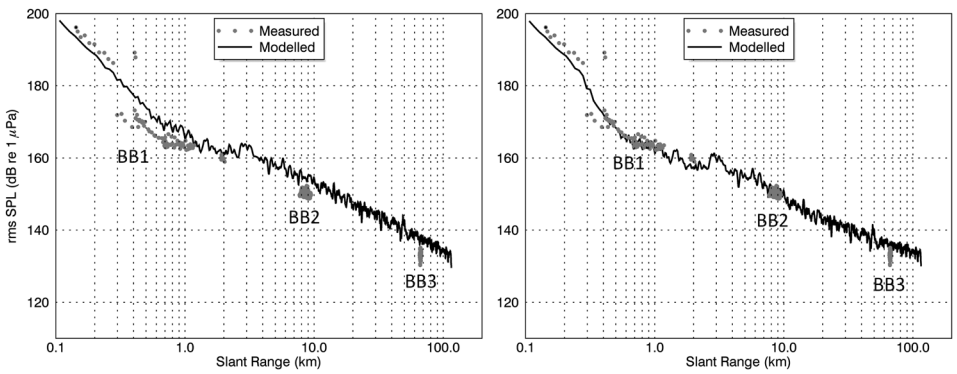

FIG. 13. Comparison of the per pulse fixed window SPL Stations BB1 to BB3 on 4 September 2012 as the *Amani* passed over the hydrophones at BB1 with the modeled outputs (left) using the pre-survey sound-speed profile, bathymetry, and SEL-SPL conversion radials, and (right) using the measured sound-speed profile, bathymetry, and SEL-SPL conversion radial from BB1 to BB3.

We compared how the peak sound pressure level and the SPL changed as the seismic source approached the recorders. The SPL was computed three ways: with a 125 ms fixed window, a 1-min fixed window, and a variable window that included 90% of the pulse energy. The 125 ms window has been shown to be near the time span over which mammalian ears integrate sound, and it applies to both terrestrial and marine mammals (Plomp and Bouman, 1959; Johnson, 1968; Kastelein *et al.*, 2010). In particular, Tougaard *et al.* (2015) transpose measurements from 11 other studies to the signal level in a 125 ms "leaky integrator" and demonstrate that the onset of disturbance using this integration time was 40–50 dB above the porpoise audiogram and closely followed the shape of the audiogram. We chose to use a fixed duration 125 ms fixed window since it is much easier to implement than the leaky integrator and has a maximum difference in calculated sound levels of 2 dB compared to the leaky integrator—a difference far smaller than the spread of SPL values associated with marine mammal disturbance (Tougaard *et al.*, 2015). The fixed window also has the advantage of estimating conservative sound levels for pulses with high initial amplitudes and long reverberant tails, such as those from seismic surveys and pile driving.

For this analysis, we choose 3.7 days of data from the 100 m deep hydrophones at Stations BB1 and BB3 during periods when only a single seismic vessel was active. Ranges to the vessels were 0.5–150 km. As expected, the results of all four methods of computing the SPL exhibited a common trend of increasing sound levels as a vessel approached a station (Fig. 14). However, each of the metrics had different slopes as a function of range, and different degrees of variability in the instantaneous variance and the deflections of the smoothing curve. The variance of the individual measurements increased with decreasing integration time, but the smoothing curves had fewer deflections. With longer integration times, there was less variance in the individual measurements, but the smoothing curve showed larger deflections, providing better insight into the average change in propagation loss as function of range. The T_{90} SPL was closer to the 125 ms SPL at short ranges, and closer to the 1-min SPL at long ranges. We expect that the variability depends on range, water depth, bottom shape, and bottom type. Therefore, the relationship between the T_{90} SPL will be more dependent on the environment than the peak sound pressure levels, 125 ms SPL and 1-min SPL, which is undesirable for a regulatory metric.

Given the variable nature of the attenuations, the data were fit with an additive model (mgcv::gam; Wood, 2004), which smoothly followed the changing sound level attenuation as a function of range (e.g., Figs. 14 and 11). The additive models were fit with 6–20 knots {e.g., gam[SPL ~ s(range, k = 20)]}. These models had much, much lower Akaike information criterion scores than linear models of the form [SPL ~ log10(range) + range] and provided a much better representation of the data. We recommend the use of additive models for predicting sound exceedance isopleths for measurement programs where the attenuation changes with range [i.e., from spherical-like spreading to cylindrical-like spreading (Fig. 11)].

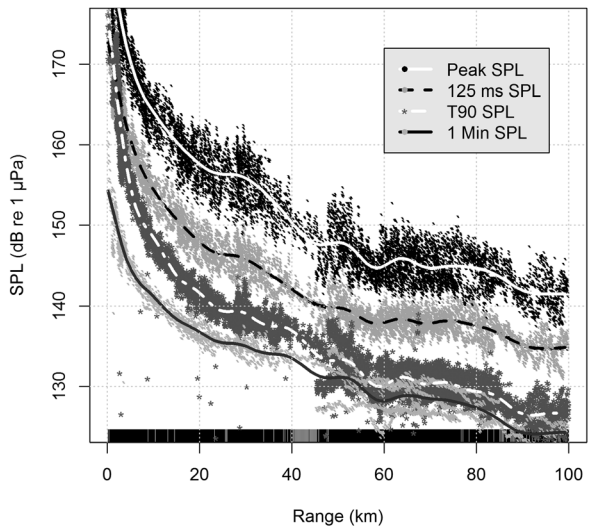

FIG. 14. Analysis of the peak SPL and SPL computed using three different averaging durations as a function of range to the source vessel. 3.7 days of data from periods when only one ship was emitting are shown; the 100 m hydrophones were used in all cases.

Additive models were generated for each averaging duration and used to compute the range where the peak SPL and SPL dropped below 120, 130, 140, 150, 160, 170, and 180 dB re 1 μPa (Table II). The ranges to the isopleths were highly dependent on the integration times. For example, the 160-dB isopleth was 48 km for the 125 ms integration time, but 26.5 km using the 90-percent energy windows and 11.6 km for 1-min integration. This result underscores the argument made in Tougaard *et al.* (2015) that measurements performed to assess compliance with a regulatory threshold must use the same metric that was used to establish that threshold. Regulatory directions and/or international standards should specify the signal analysis methods, as well as the thresholds to maximize consistency between localities and projects. Whenever possible the methods must be simple for regulators and project teams to implement. The 125 ms SPL is attractive for assessing seismic sources because (1) the duration is well matched to the length of the peak energy of the pulse in many environments; (2) it is near the length of time that the ears of many species groups integrates sound; (3) it is the fast-time weight duration in many sound

TABLE II. Radii (km) to SPL isopleths predicted by mgcv::gam additive models for the sound levels (e.g., Fig. 15) generated using 3.7 days of data from time periods when only one seismic array was active. <0.1 and >150 indicate that the result is outside the range where extrapolation is considered unreliable.

Isopleth SPL (dB re 1 μPa)	Peak sound pressure level	125 ms fixed window	T_{90} SPL	1-min SPL
180	1	<0.1	<0.1	<0.1
170	6	0.5	1.5	<0.1
160	13.8	6	3.4	<0.1
150	41.8	14.8	8.3	1.6
140	111.8	48.3	23.1	11
130	>150	>150	75.1	54.1
120	>150	>150	>150	>150

level meters; and (4) it was shown by Tougaard *et al.* (2015) to be a good predictor of the sound level at which porpoise respond to sound. We also note that the use of broadband SPL to predict behavioral reactions will likely be revisited. Like the weighted sound exposure levels used to estimate the onset of permanent threshold shift (PTS) and temporary threshold shift (TTS), we expect that audiogram-weighted SPL are better predictors of behavioral reactions.

G. Spectral content of the measured data

We need to understand the spectral content of seismic pulses propagating over long distances to inform studies on the potential for seismic surveys to disturb marine mammals that communicate at frequencies above 1 kHz or to mask their communications or foraging calls (Goold and Fish, 1998; Madsen *et al.*, 2006; Hermannsen *et al.*, 2015). The hydrophones at 100 m depth were sampled at 64 ksps; their data thus provide information on the spectral content of seismic pulses up to 30 kHz over ranges of 0.1–150 km from the seismic source. For this investigation, we used the same 3.7 days of data that were selected for the SPL investigation (Sec. III F). The peak sound pressure level as well as the broadband SPL and SPL resolved in 11 octave bands were plotted against the range to the seismic array. We computed the SPL using the 1-min (Fig. 15), 125 ms (Fig. S-11),[1] and 90% energy duration (Fig. S-12)[1] window to help illustrate the differences between these metrics.

Additive models for the peak sound pressure level, SPL, and SPL in the octave bands from 16 to 16 000 Hz were generated and used to determine where the SPL exceeded the median noise in the same band measured in September 2013 by 20 dB (Table III). Twenty decibels was chosen as a general critical ratio for detectability of signals in noise at lower frequency bands across species groups (Au and Hastings, 2008; Erbe, 2008; Gaspard *et al.*, 2012; Sills *et al.*, 2014, 2015). Using the 1-min SPL as an indication of the continuous noise from the seismic survey in Greenland waters, the range was 80 km for the 125 Hz band and decreased to 5.7 km for the 16 kHz octave band (Table III). It should be noted that the 16 kHz band integrated sound from 11 to 22 kHz; the large bandwidth increased the noise background compared to other bands, so that the noise floor of the recorder was reached at 6 km in this band (e.g., Fig. 15). For the 16 kHz band, only up to 4 km was used to generate the additive models and predicted results would have been rejected if the range exceeds 8 km. For all other bands with predicted ranges less than 150 km, the models were only interpolated and not extrapolated.

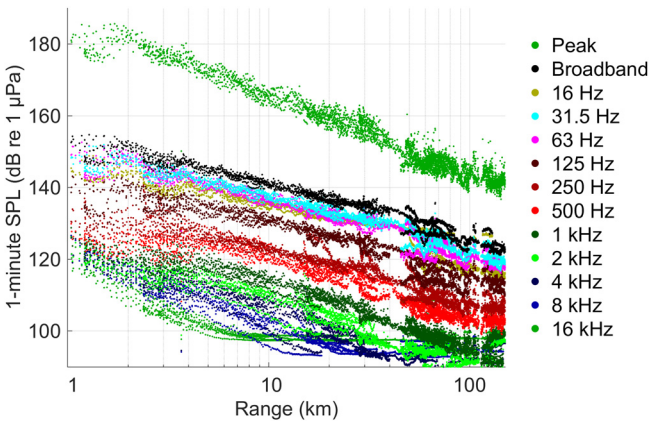

FIG. 15. (Color online) Received 1-min peak sound pressure level, broadband SPL, and octave-band SPLs (all in dB re 1 μPa) for ranges of 0.5–150 km during the 2012 Greenland survey. The 5400 min of data shown are from periods when only one seismic survey source was emitting; the 100 m hydrophones at Stations BB1 and BB3 were used in all cases. To record the high seismic sound levels without saturating the hydrophone, low sensitivity hydrophones were employed. The system spectral noise floor was 58–63 dB re 1 μPa^2/Hz, or 98–103 dB re 1 μPa broadband in the 16 kHz octave band (see Table S-3) (footnote 1). The median ambient 16 kHz octave SPL in September 2013 was 77.9 dB re 1 μPa (Fig. 5, Table S-5) (footnote 1).

TABLE III. Range from the source (km) where the seismic pulse sound levels exceed the median one-minute SPL for Sept 2013 at station BB6 by 20 dB (Table S-5) (footnote 1). The range was limited to 150 km to avoid extrapolating beyond the measured data.

	Averaging duration		
	0.125-s SPL	90% energy duration SPL	1-min SPL
Peak SPL	89.3	91.8	97.9
SPL	>150	>150	>150
Octave bands:			
16 Hz	>150	>150	>150
31 Hz	>150	>150	>150
63 Hz	>150	>150	>150
125 Hz	145.5	117.3	77.9
250 Hz	102	56.6	44.7
500 Hz	86.8	41.4	32.5
1 kHz	21	27.5	17.4
2 kHz	17.5	21.5	13.5
4 kHz	16.4	16.9	10.6
8 kHz	12.4	11.6	9.4
16 kHz	6.1	6.8	5.7

We carefully reviewed the data collection, data analysis, and sound propagation effects to verify that these high-frequency measurements were real. We conducted a detailed review of the signal analysis software and verified that the high-frequency components were not an artefact of spectral leakage in the Fourier transforms. Because the multipath features of the signals measured at 100 m and 400 m depth were very similar (Figs. 7 and 8), we are confident that the frequency content is similar throughout the water column, at least to 40 km from the source. Beyond 40 km, the high-frequency content measured on the 100 m deep hydrophones may be unrepresentative of the full water column. The hard and flat bottom conditions that we believe are responsible for the distinct multipath arrivals of the seismic pulses in Baffin Bay are also responsible in part for the long ranges where higher frequencies are still present. As noted in Sec. II C, the 100 m hydrophones were on the lower edge of the surface sound duct, so that the levels reported here are may be lower than would have been measured at 60 m.

IV. SUMMARY AND CONCLUSIONS

The Baffin Bay recordings of seismic airgun and ambient sound levels in 600–770 m water depth were analyzed to

understand the effects of a 3-D seismic survey on the acoustic environment. In 2012, data were recorded at three stations using vertical arrays with three hydrophones each; the top hydrophone at 100 m depth sampled at 64 ksps. A follow-on measurement of a shallow-hazards seismic program in 2013 and a year-long recording program overwinter in 2013–2014 showed that the soundscape in Baffin Bay is typical of open-ocean with little anthropogenic noise. The August to September soundscape closer to shore in the Melville Bay nature sanctuary is loud and dominated by the sounds of melting glacial ice.

The seismic airgun sounds measured within 40 km of the source included up to 20 distinct multipath arrivals, far more than has been reported for seismic surveys in other deep water environments. The pre-survey estimates of received sound levels were 3–7 dB higher than the levels measured for ranges of 0.5–65 km. The error between the measured and modelled sound levels decreased to 0–4 dB by using the sound speed profile, bathymetry, and modeling along the same radial as was measured.

When the vessel was closer to a station than 40 km, there was virtually no difference in the daily SEL as a function of depth; however, there were short-term variations in per-pulse SEL and SPL on the order of 6 dB. At ranges of 40 km from the seismic source, the difference in levels as a function of depth became significant. At 40 km, the SPL was generally below 140 dB re 1 μPa, which is well below the levels associated with risk of injury to marine life. In the project area, the sound speed profile below 400 m is either iso-velocity or downward refracting. Thus, measuring at the seabed would have provided similar information within 40 km of the source as we measured with the vertical arrays. For future monitoring projects in similar environments, we recommend collecting data at the seafloor only (assuming a downward refracting sound speed profile), which will allow for simpler moorings that are lower cost and easier to deploy and retrieve. These types of moorings have the added advantage of exhibiting lower levels of flow induced pseudo-noise since most locations have little current at the seafloor.

The measured sound levels were compared to several proposed regulatory thresholds for auditory injury. Using the frequency weighting functions and thresholds recommended in Southall *et al.* (2007), which were incorporated into the *Guidelines to Environmental Impact Assessment of Seismic Activities in Greenland Waters,* we estimated the threshold of injury for low-frequency cetaceans at a range of <100 m and for phocids (seals) at a range of 600 m. These ranges agreed with the maximum expected ranges from the pre-survey modeling.

We noted that the SPL is a difficult metric to employ for regulatory thresholds, however, it remains in use for many purposes and demonstrated how the SPL depends on the integration time. We compared the SPL computed using two fixed window durations (125 ms and 1 min) with the SPL computed using 90% energy duration of the seismic pulses. The sound levels did not smoothly decrease as a function of range with any of the metrics and were best described using an additive model rather than a linear regression. We found that the integration time affects what information we extract from the data. Unsurprisingly, shorter integration times provide better information on the instantaneous variance in the signal, while longer integration times smooth the variance and reveal longer-term effects. The peak sound pressure level, 125 ms SPL, and 1-min SPL curves tracked each other while the T_{90} SPL was closer to the 125 ms SPL at short range and close to the 1-min SPL at long range. Thus, the T_{90} SPL depends on the environment more strongly than the fixed integration windows and is not recommended for establishing regulatory thresholds. If the SPL must be used for characterizing the effects of sound on marine life, we suggest standardizing on the 125 ms window for seismic sources.

The Baffin Bay recordings confirm previous reports that seismic airgun sounds include energy up to at least 30 kHz. The SPL in the band used by dolphin species for social whistle communications (16 kHz octave band) were increased by 20 dB compared to the ambient levels measured in September 2013 at ranges of 6 km from the source vessels for all integration durations.

The collection and analysis of this dataset has produced a wealth of new information on the Baffin Bay environment and the variability of seismic array sound propagation. This study shows the importance of collecting systematic data during industrial operations when there are uncertainties in the possible effects of the activity on the acoustic environment. Future projects can extend this work by verifying the dependence of the multipath arrivals and high-frequency content on the bottom composition and depth, investigating the azimuthal characteristics of a seismic array, exploring the variation in sound levels with depth in different environments, and attempting to measure the behavioral reactions of marine life as a function of range to the seismic source.

ACKNOWLEDGMENTS

The authors would like to thank Shell Global Solutions for making this data set available for publication and JASCO Applied Sciences for their support of the manuscript preparation. We also thank JASCO's engineering and field teams for developing and deploying the vertical moorings that successfully recorded this data set. Brad Boschetto (Shell International Exploration and Production) made helpful contributions to the initiation and execution of the project. Reviews by Mikhail Zykov, Roberto Racca, Peter van der Sman, David Barclay, and our anonymous reviewers contributed to the strength and readability of this manuscript. Finally, thanks to Karen Hiltz for her patient reviews and edits to the manuscript.

[1]See supplementary material at https://doi.org/10.1121/1.5014049 for the additional figures and tables referenced in this manuscript.

ANSI S1.4-1983 (**2006**). "American national standard specification for sound level meters" (American National Standards Institute, New York).

Au, W. W. L., and Hastings, M. C. (**2008**). *Principles of Marine Bioacoustics* (Springer, New York).

Blackwell, S. B., Lawson, J. W., and Williams, M. T. (**2004**). "Tolerance by ringed seals (*Phoca hispida*) to impact pipe-driving and construction sounds at an oil production island," J. Acoust. Soc. Am. **115**, 2346–2357.

Blackwell, S. B., Nations, C. S., McDonald, T. L., Thode, A. M., Mathias, D., Kim, K. H., Greene, C. R., Jr., and Macrander, A. M. (**2015**). "Effects of airgun sounds on bowhead whale calling rates: Evidence for two behavioral thresholds," PLoS One **10**, e0125720.

Bohnenstiehl, D. R., Howell, J. K., White, S. M., and Hey, R. N. (**2012a**). "A modified basal outlining algorithm for identifying topographic highs from gridded elevation data, Part 1: Motivation and methods," Comput. Geosci. **49**, 308–314.

Bohnenstiehl, D. R., Scheip, C. M., Matsumoto, H., and Dziak, R. P. (**2012b**). "Acoustics variability of air gun signals recorded at intermediate ranges within the Lau Basin," Geochem. Geophys. Geosyst. **13**, Q11013.

Breitzke, M., and Bohlen, T. (**2010**). "Modelling sound propagation in the Southern Ocean to estimate the acoustic impact of seismic research surveys on marine mammals," Geophys. J. Int. **181**, 818–846.

Caldwell, J., and Dragoset, W. (**2000**). "A brief overview of seismic air-gun arrays," Leading Edge **19**, 898–902.

Carroll, A. G., Przeslawski, R., Duncan, A., Gunning, M., and Bruce, B. (**2017**). "A critical review of the potential impacts of marine seismic surveys on fish & invertebrates," Mar. Pollut. Bull. **114**, 9–24.

Cato, D. H. (**2008**). "Ocean ambient noise: Its measurement and its significance to marine animals," Proc. Inst. Acoust. **30**, 1–9.

Clark, C. W., Ellison, W. T., Southall, B. L., Hatch, L., Van Parijs, S. M., Frankel, A., and Ponirakis, D. (**2009**). "Acoustic masking in marine ecosystems: Intuitions, analysis, and implication," Mar. Ecol. Prog. Ser. **395**, 201–222.

Collins, M. D. (**1993**). "A split-step Padé solution for the parabolic equation method," J. Acoust. Soc. Am. **93**, 1736–1742.

Deruiter, S. L., Southall, B. L., Calambokidis, J., Zimmer, W. M., Sadykova, D., Falcone, E. A., Friedlaender, A. S., Joseph, J. E., Moretti, D., Schorr, G. S., Thomas, L., and Tyack, P. L. (**2013**). "First direct measurements of behavioural responses by Cuvier's beaked whales to mid-frequency active sonar," Biol. Lett. **9**, 1–5.

Dragoset, W. H. (**1990**). "Air-gun array specs: A tutorial," Leading Edge **9**, 24–32.

Ellison, W. T., Southall, B. L., Clark, C. W., and Frankel, A. S. (**2012**). "A new context-based approach to assess marine mammal behavioral responses to anthropogenic sounds," Conserv. Biol. **26**, 21–28.

Erbe, C. (**2008**). "Critical ratios of beluga whales (*Delphinapterus leucas*) and masked signal duration," J. Acoust. Soc. Am. **124**, 2216–2223.

Finneran, J. J., and Jenkins, A. K. (**2012**). "Criteria and thresholds for U.S. Navy acoustic and explosive effects analysis" (SPAWAR Systems Center Pacific, San Diego, CA).

Frouin-Mouy, H., Kowarski, K., Martin, B., and Bröker, K. (**2017**). "Seasonal trends in acoustic detection of marine mammals in Baffin Bay and Melville Bay, Northwest Greenland + supplementary appendix 1," Arctic **70**, 18.

Frouin-Mouy, H., Mouy, X., Martin, B., and Hannay, D. (**2015**). "Underwater acoustic behavior of bearded seals (*Erignathus barbatus*) in the northeastern Chukchi Sea, 2007–2010," Mar. Mamm. Sci **32**(1), 141–160.

Gaspard, J. C., III, Bauer, G. B., Reep, R. L., Dziuk, K., Cardwell, A., Read, L., and Mann, D. A. (**2012**). "Audiogram and auditory critical ratios of two Florida manatees (*Trichechus manatus latirostris*)," J. Exp. Biol. **215**, 1442–1447.

Gedamke, J., Gales, N., and Frydman, S. (**2011**). "Assessing risk of baleen whale hearing loss from seismic surveys: The effect of uncertainty and individual variation," J. Acoust. Soc. Am. **129**, 496–506.

Gisiner, B. (**2016**). "Sound and marine seismic surveys," Acoust. Today **12**(4), 9–18.

Goldbogen, J. A., Southall, B. L., Deruiter, S. L., Calambokidis, J., Friedlaender, A. S., Hazen, E. L., Falcone, E. A., Schorr, G. S., Douglas, A., Moretti, D. J., Kyburg, C., McKenna, M. F., and Tyack, P. L. (**2013**). "Blue whales respond to simulated mid-frequency military sonar," Proc. R. Soc. B **280**, 20130657.

Goold, J. C., and Fish, P. J. (**1998**). "Broadband spectra of seismic survey air-gun emissions, with reference to dolphin auditory thresholds," J. Acoust. Soc. Am. **103**, 2177–2184.

Gordon, J., Gillespie, D., Potter, J., Frantzis, A., Simmonds, M. P., Swift, R., and Thompson, D. (**2003**). "A review of the effects of seismic surveys on marine mammals," Mar. Technol. Soc. J. **37**, 16–34.

Guan, S., Vignola, J., Judge, J., and Turo, D. (**2015**). "Airgun inter-pulse noise field during a seismic survey in an Arctic ultra shallow marine environment," J. Acoust. Soc. Am. **138**, 3447–3457.

Guerra, M., Thode, A. M., Blackwell, S. B., and Michael Macrander, A. (**2011**). "Quantifying seismic survey reverberation off the Alaskan North Slope," J. Acoust. Soc. Am. **130**, 3046–3058.

Hermannsen, L., Tougaard, J., Beedholm, K., Nabe-Nielsen, J., and Madsen, P. T. (**2015**). "Characteristics and propagation of airgun pulses in shallow water with implications for effects on small marine mammals," PLoS One **10**, e0133436.

Hildebrand, J. A. (**2009**). "Anthropogenic and natural sources of ambient noise in the ocean," Mar. Ecol. Prog. Ser. **395**, 5–20.

Johnson, C. S. (**1968**). "Relation between absolute threshold and duration-of-time pulses in the bottlenosed porpoise," J. Acoust. Soc. Am. **43**, 757–763.

Kaiser, J. F. (**1990**). "On a simple algorithm to calculate the 'energy' of a signal," in *International Conference on Acoustics, Speech, and Signal Processing* (IEEE, New York), pp. 381–384.

Kastelein, R. A., Hoek, L., de Jong, C. A. F., and Wensveen, P. J. (**2010**). "The effect of signal duration on the underwater detection thresholds of a harbor porpoise (*Phocoena phocoena*) for single frequency-modulated tonal signals between 0.25 and 160 kHz," J. Acoust. Soc. Am. **128**, 3211–3222.

Kastelein, R. A., Steen, N., Gransier, R., and De Jong, A. (**2013a**). "Brief behavioral response threshold level of a harbor porpoise (*Phocoena phocoena*) to an impulsive sound," Aquat. Mamm. **39**, 315–323.

Kastelein, R. A., van Heerden, D., Gransier, R., and Hoek, L. (**2013b**). "Behavioral responses of a harbor porpoise (*Phocoena phocoena*) to playbacks of broadband pile driving sounds," Mar. Environ. Res. **92**, 206–214.

Kyhn, L. A., Boertmann, D., Tougaard, J., Johansen, K., and Mosbech, A. (**2011**). "Guidelines to environmental impact assessment of seismic activities in Greenland waters," 3rd revised ed., December 2011 (Danish Center for Environment and Energy), p. 61.

Leggat, L. J., Merklinger, H. M., and Kennedy, J. L. (**1981**). "LNG carrier underwater noise study for Baffin Bay" (Defence Research Establishment Atlantic, Dartmouth, Nova Scotia), p. 32.

MacGillivray, A. O. (**2006**). "Acoustic modelling study of seismic airgun noise in Queen Charlotte Basin" (University of Victoria, Victoria, BC), p. 98.

MacGillivray, A. O. (**2013**). "A model for underwater sound levels generated by marine impact pile driving," J. Acoust. Soc. Am. **134**, 4024.

MacGillivray, A. O., Racca, R., and Li, Z. (**2014**). "Marine mammal audibility of selected shallow-water survey sources," J. Acoust. Soc. Am. **135**, EL35–EL40.

Madsen, P. T. (**2005**). "Marine mammals and noise: Problems with root mean square sound pressure levels for transients," J. Acoust. Soc. Am. **117**, 3952–3957.

Madsen, P. T., Johnson, M., Miller, P. J. O., Aguilar Soto, N., Lynch, J., and Tyack, P. (**2006**). "Quantitative measures of air-gun pulses recorded on sperm whales (*Physeter macrocephalus*) using acoustic tags during controlled exposure experiments," J. Acoust. Soc. Am. **120**, 2366–2379.

Matthews, M.-N. R. (**2012**). "Underwater sound propagation from an airgun array in Baffin Bay: Shell 2012 seismic surveys in Baffin Bay blocks 5 & 8" (Technical report for LGL Ltd., Environmental Research Associates by JASCO Applied Sciences).

Matthews, M.-N. R. (**2013**). "Underwater sound propagation from an airgun array in Baffin Bay: Shell 2013 seismic surveys in Baffin Bay, blocks 5 & 8" (Version 2.0. Technical report by JASCO Applied Sciences Ltd. for Shell Global Solutions International B. V.).

Merchant, N. D., Fristrup, K. M., Johnson, M. P., Tyack, P. L., Witt, M. J., Blondel, P., and Parks, S. E. (**2015**). "Measuring acoustic habitats," Methods Ecol. Evol. **6**, 257–265.

Miller, P., Kvadsheim, P., Lam, F., Tyack, P. L., Curé, C., DeRuiter, S. L., Kleivane, L., Sivle, L., van IJsselmuide, S., and Visser, F. (**2015**). "First indications that northern bottlenose whales are sensitive to behavioural disturbance from anthropogenic noise," R. Soc. Open Sci. **2**, 140484.

National Marine Fisheries Service (**2016**). "Technical guidance for assessing the effects of anthropogenic sound on marine mammal hearing: Underwater acoustic thresholds for onset of permanent and temporary threshold shifts" (U.S. Department of Commerce, NOAA Technical Memorandum NMFS-OPR-55), p. 178.

National Oceanic and Atmospheric Administration (**2013**). "Effects of oil and gas activities in the Arctic Ocean: Supplemental draft environmental impact statement" (prepared by United States Department of Commerce, National Oceanic and Atmospheric Administration, National Marine Fisheries Service, Office of Protected Resources), p. 60.

National Research Council (**2005**). *Marine Mammal Populations and Ocean Noise: Determining when Ocean Noise Causes Biologically Significant Effects* (National Academy Press, Washington, DC), 142 pp.
Nieukirk, S. L., Mellinger, D. K., Moore, S. E., Klinck, K., Dziak, R. P., and Goslin, J. (**2012**). "Sounds from airguns and fin whales recorded in the mid-Atlantic Ocean, 1999–2009," J. Acoust. Soc. Am. **131**, 1102–1112.
Nowacek, D. P., Bröker, K., Donovan, G., Gailey, G., Racca, R., Reeves, R. R., Vedenev, A. I., Weller, D. W., and Southall, B. L. (**2013**). "Responsible practices for minimizing and monitoring environmental impacts of marine seismic surveys with an emphasis on marine mammals," Aquat. Mamm. **39**, 356–377.
Nowacek, D. P., Thorne, L. H., Johnston, D. W., and Tyack, P. L. (**2007**). "Responses of cetaceans to anthropogenic noise," Mamm. Rev. **37**, 81–115.
Pettit, E. C., Lee, K. M., Brann, J. P., Nystuen, J. A., Wilson, P. S., and O'Neel, S. (**2015**). "Unusually loud ambient noise in tidewater glacier fjords: A signal of ice melt," Geophys. Res. Lett. **42**, 2309–2316, https://doi.org/10.1002/2014GL062950.
Pirotta, E., Milor, R., Quick, N., Moretti, D., Di Marzio, N., Tyack, P., Boyd, I., and Hastie, G. (**2012**). "Vessel noise affects beaked whale behavior: Results of a dedicated acoustic response study," PLoS One **7**, e42535.
Plomp, R., and Bouman, M. A. (**1959**). "Relation between hearing threshold and duration for tone pulses," J. Acoust. Soc. Am. **31**, 749–758.
Popper, A. N., Hawkins, A. D., Fay, R. R., Mann, D. A., Bartol, S., Carlson, T. J., Coombs, S., Ellison, W. T., Gentry, R. L., and Halvorsen, M. B. (**2014**). "Sound exposure guidelines," in *ASA S3/SC1. 4 TR-2014 Sound Exposure Guidelines for Fishes and Sea Turtles: A Technical Report prepared by ANSI-Accredited Standards Committee S3/SC1 and registered with ANSI* (Springer, New York), pp. 33–51.
Richardson, W. J., Würsig, B., and Greene, C. R., Jr. (**1986**). "Reactions of bowhead whales, *Balaena mysticetus*, to seismic exploration in the Canadian Beaufort Sea," J. Acoust. Soc. Am. **79**, 1117–1128.
Risch, D., Corkeron, P. J., Ellison, W. T., and Van Parijs, S. M. (**2012**). "Changes in humpback whale song occurrence in response to an acoustic source 200 km away," PLoS One **7**, e29741.
Robertson, F. C., Koski, W. R., Thomas, T. A., Richardson, W. J., Würsig, B., and Trites, A. W. (**2013**). "Seismic operations have variable effects on dive-cycle behavior of bowhead whales in the Beaufort Sea," Endangered Species Res. **21**, 143–160.
Rodriguez, E., Morris, C. S., Belz, Y. J. E., Chapin, E. C., Martin, J. M., Daffer, W., and Hensley, S. (**2005**). "An assessment of the SRTM topographic products" (Jet Propulsion Laboratory Pasadena, CA).
Roth, E. H., Hildebrand, J. A., and Wiggins, S. M. (**2012**). "Underwater ambient noise on the Chukchi Sea continental slope from 2006–2009," J. Acoust. Soc. Am. **131**, 104–110.
Sabra, K., Cornuelle, B., and Kuperman, B. (**2016**). "Sensing deep-ocean temperatures," Phys. Today **69**(2), 32–38.
Shannon, G., McKenna, M. F., Angeloni, L. M., Crooks, K. R., Fristrup, K. M., Brown, E., Warner, K. A., Nelson, M. D., White, C., Briggs, J., McFarland, S., and Wittemyer, G. (**2016**). "A synthesis of two decades of research documenting the effects of noise on wildlife," Biol. Rev. **91**, 982–1005.
Sills, J. M., Southall, B. L., and Reichmuth, C. (**2014**). "Amphibious hearing in spotted seals (*Phoca largha*): Underwater audiograms, aerial audiograms and critical ratio measurements," J. Exp. Biol. **217**, 726–734.
Sills, J. M., Southall, B. L., and Reichmuth, C. (**2015**). "Amphibious hearing in ringed seals (*Pusa hispida*): Underwater audiograms, aerial audiograms and critical ratio measurements," J. Exp. Biol. **218**, 2250–2259.
Southall, B. L., Bowles, A. E., Ellison, W. T., Finneran, J. J., Gentry, R. L., Greene, C. R., Jr., Kastak, D., Ketten, D. R., Miller, J. H., Nachtigall, P. E., Richardson, W. J., Thomas, J. A., and Tyack, P. L. (**2007**). "Marine mammal noise exposure criteria: Initial scientific recommendations," Aquat. Mamm. **33**, 411–521.
Tashmukhambetov, A. M., Ioup, G. E., Ioup, J. W., Sidorovskaia, N. A., and Newcomb, J. J. (**2008**). "Three-dimensional seismic array characterization study: Experiment and modeling," J. Acoust. Soc. Am. **123**, 4094–4108.
Teague, W. J., Carron, M. J., and Hogan, P. J. (**1990**). "A comparison between the generalized digital environmental model and levitus climatologies," J. Geophys. Res. **95**, 7167–7183, https://doi.org/10.1029/JC095iC05p07167.
Thode, A., Kim, K. H., Greene, C. R., Jr., and Roth, E. (**2010**). "Long range transmission loss of broadband seismic pulses in the Arctic under ice-free conditions," J. Acoust. Soc. Am. **128**, EL181–EL187.
Tougaard, J., Wright, A. J., and Madsen, P. T. (**2015**). "Cetacean noise criteria revisited in the light of proposed exposure limits for harbour porpoises," Mar. Pollut. Bull. **90**, 196–208.
Urick, R. J. (**1983**). *Principles of Underwater Sound* (McGraw-Hill, New York).
Wartzok, D., Popper, A. N., Gordon, J., and Merrill, J. (**2003**). "Factors affecting the responses of marine mammals to acoustic disturbance," Mar. Technol. Soc. J. **37**, 6–15.
Wisniewska, D. M., Kyhn, L. A., Tougaard, J., Simon, M., Lin, Y.-T., Newhall, A., Beedholm, K., Lynch, J., and Madsen, P. T. (**2014**). "Propagation of airgun pulses in Baffin Bay 2012," in Scientific report from DCE—Danish Centre for Environment and Energy.
Wood, J., Southall, B. L., and Tollit, D. J. (**2012**). "PG&E offshore 3 D seismic survey project EIR-marine mammal technical draft report" (SMRU Ltd).
Wood, S. N. (**2004**). "Stable and efficient multiple smoothing parameter estimation for generalized additive models," J. Am. Stat. Assoc. **99**, 673–686.